

Light-to-light transducers integrated with heterojunction phototransistors and a laser diode

Susumu Noda, Kimitaka Shibata and Akio Sasaki

Department of Electrical Engineering, Kyoto University, Kyoto 606 (Japan)

(Received February 15, 1993, in revised form August 12, 1993)

Abstract

A semiconductor light-to-light transducer has been developed by vertical and direct integration of heterojunction phototransistors and a laser diode. The transducer detects an optical signal and emits an intensified optical output. A linear amplification with gain > 100 for input light of $0\text{--}30 \mu\text{W}$ is achieved by the suppression of internal optical feedback. The static intensity noise properties of the transducer are also investigated theoretically. It is estimated that the noise equivalent power is 30 pW , and the relative intensity noise for a typical input power level of $\sim 10 \mu\text{W}$ is about $10^{-14}\text{--}10^{-13}$.

1. Introduction

A light-to-light transducer has been reported as a new type of radiation transducer with various functions [1, 2]. It is considered as a device that detects light signals, converts them to electrical signals, amplifies them, and emits the intensified light signals. The device has various functions, such as optical amplification, bistability, and switching. Therefore, the light-to-light transducer can be considered as a key device for optical sensing as well as for optical signal processing and optical computing.

Thus far, the light-to-light transducer has been made by the vertical and direct integration of a heterojunction phototransistor (HPT) and a light-emitting diode (LED). The device is considered as a kind of optoelectronic integrated device (OEID) rather than an optoelectronic integrated circuit (OEIC) [2]. In this work, we have developed a light-to-light transducer by the vertical and direct integration of heterojunction phototransistors and a laser diode (LD). The LD offers various attractive features, such as higher differential quantum efficiency, emission of coherent light, thresholding characteristics, and so on, compared with the case of the LED [3].

In the following Sections, the structure, fabrication procedure, and characteristics of the transducer are described. Among various light-to-light transducing characteristics, the linear optical amplification characteristics are especially emphasized and the theoretical analysis of the noise properties is also given, since these are important for sensing performance.

2. Structure of light-to-light transducer

Figure 1 shows the schematic structure of a light-to-light transducer. The device is composed of three HPTs and an LD with a p-substrate buried crescent (PBC) configuration [4].

The crystal wafer for the device was grown by three-step liquid-phase epitaxy (LPE). The current-blocking layers of p-InP ($p=7 \times 10^{17} \text{ cm}^{-3}$, thickness $d=2 \mu\text{m}$), n-InP ($n=4 \times 10^{17} \text{ cm}^{-3}$, $d=0.7 \mu\text{m}$), and p-InP ($p=7 \times 10^{17} \text{ cm}^{-3}$, $d=1.7 \mu\text{m}$) were grown on a p-InP substrate at the first LPE. The p-InP cladding ($p=7 \times 10^{17} \text{ cm}^{-3}$, $d \approx 1 \mu\text{m}$), undoped InGaAsP active (band-gap wavelength $\lambda=1.3 \mu\text{m}$, $d=0.2 \mu\text{m}$), n-InP cladding ($n=7 \times 10^{17} \text{ cm}^{-3}$, $d=3.0 \mu\text{m}$), and n-InGaAsP absorptive ($\lambda=1.2 \mu\text{m}$, $n=2 \times 10^{18} \text{ cm}^{-3}$, $d=1.0 \mu\text{m}$) layers were grown at the second LPE after the formation of a groove with $2 \mu\text{m}$ width on the wafer. A laser diode with the PBC configuration was obtained by these growth processes. The HPT composed of n-InP buffer

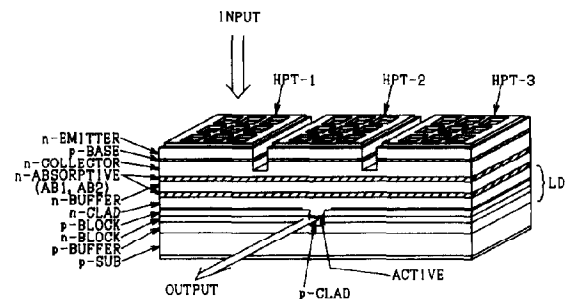


Fig 1 Schematic structure of a light-to-light transducer

($n=1 \times 10^{18} \text{ cm}^{-3}$, $d=1.6 \mu\text{m}$), n-InP absorptive ($\lambda=1.2 \mu\text{m}$, $n=1 \times 10^{18} \text{ cm}^{-3}$, $d=1.0 \mu\text{m}$), n-InP collector layer ($n=1 \times 10^{17} \text{ cm}^{-3}$, $d=4 \mu\text{m}$), p-InGaAsP base ($\lambda=1.2 \mu\text{m}$, $p=5 \times 10^{16} \text{ cm}^{-3}$, $d=0.4 \mu\text{m}$), and n-InP emitter ($n=1 \times 10^{18} \text{ cm}^{-3}$, $d=1.0 \mu\text{m}$) layers was grown at the third LPE

After the growth, a mesh AuGe/Ni/Au electrode was evaporated on the epilayer side, and the wafer was mesa-etched to form three HPTs. The AuZn/Au electrode was deposited on the backside of the substrate. The wafer was then cleaved and bonded on a silver heat sink. The dimensions of each HPT were $210 \times 290 \mu\text{m}^2$, and the cavity length of the LD was $290 \mu\text{m}$.

3. Characteristics of light-to-light transducer

Since the transducer has three HPTs on a single LD, various light-to-light transducing characteristics can be obtained by various combinations of one of the three HPTs and the LD. When HPT-2 is utilized as the HPT part, it is greatly affected by optical feedback from the LD. This induces a sharp negative resistance characteristic in the current-voltage characteristics. By utilizing this negative resistance characteristic, a high gain and very sensitive photonic switching have been achieved, as reported previously [3]. In this case, however, the linearity between the output and input light signal powers is lost.

When linearity between the input and output powers is required, optical feedback from the LD to the HPT should be suppressed. For the purpose, HPT-1 was utilized as the HPT portion, where the relative separation of HPT-1 and the LD was increased. The distance between the stripe of the LD and the edge of HPT-1 was $185 \mu\text{m}$. Here we note that the optical absorptive layers AB1 and AB2 were present between the HPT and the LD to achieve additional suppression of the feedback.

The threshold current of the LD part was 42 mA under cw conditions at room temperature, and the differential quantum efficiency was 11% for one facet. The output wavelength was $1.29 \mu\text{m}$ and the spontaneous emission was well saturated at the threshold current. On the other hand, the conversion gain of the HPT was ~ 1000 with a bias voltage of 4.0 V and a load resistance of 60Ω , where the input light wavelength was $1.15 \mu\text{m}$.

The current-voltage characteristics of the transducer are shown in Fig. 2, where the input light ($\lambda_{in}=1.15 \mu\text{m}$) power is taken as a parameter. A negative differential resistive characteristic is not seen in Fig. 2, except for the case $P_{in}=0 \mu\text{W}$. It is considered that substantial optical feedback does not occur in the device composed of HPT-1 and the LD. The negative char-

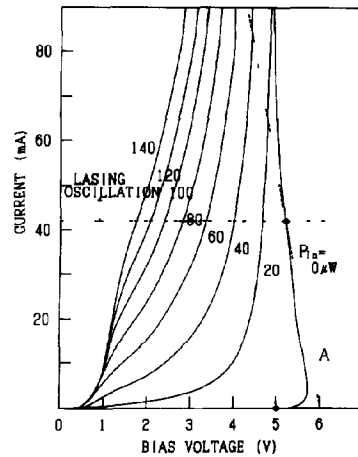


Fig. 2 Current-voltage characteristics of the transducer, where the input light power is taken as a parameter.

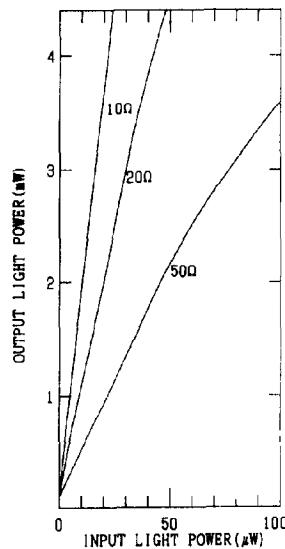


Fig. 3 Output-input light-signal power characteristics, where the load resistance is taken as a parameter.

acteristic appears in the dark condition ($P_{in}=0 \mu\text{W}$) due to the Early effect and the avalanche multiplication effect in the HPT-1 itself.

The dark current can be utilized to pre-bias the transducer just at the threshold current of the LD part. When the broken line shown in Fig. 2 was selected as the load line, which passes through the threshold current under the dark condition, the output-input light-power characteristics became as shown in Fig. 3, where the load resistance R is taken as a parameter. It is seen in Fig. 3 that a fairly good linear relationship between the input and output power characteristics has been obtained, especially at $R=10 \Omega$. When $R=10 \Omega$, the optical gain was as high as ~ 200 . The dependence of

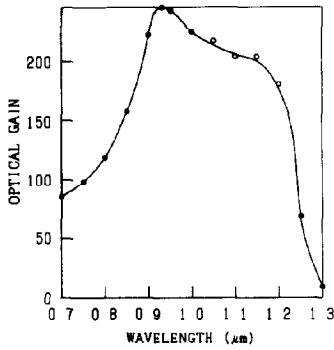


Fig 4 Dependence of optical gain on input light wavelength

the optical gain on the input light wavelength is shown in Fig 4. An optical gain over 100 has been achieved in the wide wavelength range 0.75–1.25 μm . When the input wavelength was 0.92 μm , the optical gain was 250, the highest ever reported for this type of light-to-light transducer. The large gain is due to the achievement of lasing oscillation in the light-emitting part and also to the realization of a high conversion gain in the light-receiving part. The rise and fall times of the transducer were ~ 500 ns and ~ 800 ns, respectively, and were obtained by the pulse-response measurement. They can be made faster by reducing the surface area of the HPT to decrease the CR constant. A response time of about 10 ns may be possible when the surface area becomes $25 \times 25 \mu\text{m}^2$.

It is seen in Fig 3 that the transducer emitted about 150 μW output light power even when $P_{\text{in}} = 0$. This is due to spontaneous emission with a broad spectral linewidth, this can be removed by using a narrow-bandwidth optical filter that can only pass the lasing oscillation mode. The optical filter is also important to reduce the intensity noise of the transducer, as described in the next Section.

4. Relative intensity noise

In Section 3, we described the experimental results on the linear amplification of detecting optical signals. Here we discuss theoretically the intensity noise properties of the transducer. Noise properties are important for the application of the transducer to various sensor systems.

The analysis was made by using the rate equations for the LD, and the shot noise coming from the HPT was considered. We derive here the static relative intensity noise, defined as $RIN = \langle \delta P^2 \rangle / P_0^2$ for the continuous-wave optical input signal to the transducer, where δP and P_0 are the fluctuation and the mean value of the output signal from the transducer, respectively. Note that we do not treat the dynamic noise

properties here. We assumed that the LD oscillates in a single longitudinal mode and that the carrier avalanche effect does not occur in the HPT.

The rate equation for carrier numbers n in an active layer is expressed as

$$\frac{dn}{dt} = -\frac{n}{\tau_s} - G_{\text{LD}}(n)S + \frac{I}{q} + F_n(t) \quad (1)$$

where τ_s denotes the carrier lifetime, $G_{\text{LD}}(n)$ the modal gain of an LD, S the photon numbers, q the magnitude of the electron charge, and F_n the fluctuation of the carrier numbers. I is the injection current, given by

$$I = \frac{qG_{\text{HPT}}}{h\nu} P_{\text{in}} \quad (2)$$

where $h\nu$ is the photon energy of the input light and P_{in} the input light power. G_{HPT} is the conversion gain of the HPT and its frequency dependence is expressed as

$$G_{\text{HPT}} = \left(1 + \frac{G_0^2}{1 + (ff_c)^2} \right)^{1/2} \quad (3)$$

where G_0 is the conversion gain at the low-frequency region, and f_c is the cut-off frequency.

On the other hand, the rate equation for photon numbers S in an active layer is expressed as

$$\frac{dS}{dt} = G(n)S - \frac{S}{\tau_{\text{ph}}} + \beta \frac{n}{\tau_s} + F_S(t) \quad (4)$$

where τ_{ph} is the photon lifetime, β the spontaneous emission factor, and F_S the fluctuation of the photon numbers.

The carrier and photon numbers are expressed as the sum of the mean value and the fluctuation around it

$$n = n_0 + \delta n \quad (5)$$

$$S = S_0 + \delta S \quad (6)$$

When the transducer is at the lasing oscillation condition, the average carrier number n_0 is fixed to the lasing-threshold carrier number n_{th} . We derive the time-derivative equations for δn and δS by using eqns (1), (4), (5), and (6)

$$\frac{d}{dt} \delta n = a_1 \delta n + a_2 \delta S + F_n(t) \quad (7)$$

$$\frac{d}{dt} \delta S = a_3 \delta n + F_S(t) \quad (8)$$

where the equations have been linearized by neglecting the products of fluctuations such as $\delta n \delta S$. Here

$$a_1 = -\frac{1}{\tau_s} - gS_0 \quad (9)$$

$$a_2 = -\frac{1}{\tau_{ph}} \quad (10)$$

$$a_3 = gS_0 + \frac{\beta}{\tau_s} \quad (11)$$

In the above equations, we have used the following expression for $G_{LD}(n)$

$$\begin{aligned} G_{LD}(n) &= G_{LD}(n_0 + \delta n) = G_{LD}(n_{th} + \delta n) = G_{LD}(n_{th}) + g\delta n \\ &= \frac{1}{\tau_{ph}} + g\delta n \end{aligned} \quad (12)$$

where g is the modal differential gain

The relative intensity noise (RIN) for photons can be obtained by Fourier transformation of eqns (7) and (8) as

$$\begin{aligned} RIN &= \frac{\langle \delta P^2(\omega) \rangle}{P_0^2} = \frac{\langle \delta S^2(\omega) \rangle}{S_0^2} = \\ &= \frac{a_3^2 \langle F_n^2(\omega) \rangle + (a_1^2 + \omega^2) \langle F_s^2(\omega) \rangle - 2a_1 a_3 \langle F_n(\omega) F_s(\omega) \rangle}{S_0^2 [(a_2 a_3 + \omega^2)^2 + \omega^2 a_1^2]} \end{aligned} \quad (13)$$

Here the fluctuation terms for the carrier numbers and the photon numbers are expressed as follows by using eqns (1) and (4) [5] and by considering the shot noise of the HPT [6] and the relative intensity noise $RIN(INPUT)$ of the input light signal

$$\begin{aligned} \langle F_n^2(\omega) \rangle &= \left(\frac{n_0}{\tau_s} + \frac{S_0}{\tau_{ph}} + \frac{I}{q} \right) + \frac{2I[1 + 2G_0/(1 + (f/f_c)^2)]}{q} \\ &+ \frac{[P_{in}^2 RIN(INPUT)] G_{HPT}^2}{(h\nu)^2} \end{aligned} \quad (14)$$

$$\langle F_s^2(\omega) \rangle = \frac{2S_0}{\tau_{ph}} + \beta \frac{n_{th}}{\tau_s} \quad (15)$$

$$\langle F_n(\omega) F_s(\omega) \rangle = -\frac{S_0}{\tau_{ph}} \quad (16)$$

where the second and third terms of eqn (14) express the shot noise of the HPT and the noise coming from the input light itself, respectively

Equation (13), together with the other equations, is the sought-after expression for the relative intensity noise, and we can calculate the intensity noise of the transducer. Here $n_0 = n_{th}$ and S_0 are calculated by the following equations, which are obtained from eqns (1) and (4)

$$n_0 = n_{th} = \frac{\tau_s I_{th}}{q} \quad (17)$$

$$S_0 = \frac{\tau_{ph} I_{th}}{q} R \quad (18)$$

where $R = (I - I_{th})/I_{th}$ and I_{th} is the lasing threshold current of the LD part. By utilizing eqns (17) and (18) and the relationship $gn_{th} = 1/\tau_{ph}$ [7], eqns (9)–(11) and (14)–(16) become more suitable forms for calculation. The numerical parameters used for the calculation are summarized in Table 1.

Now we shall describe the calculated results. First of all, the input light-signal power (P_{in}) dependence of RIN is discussed. Figure 5 shows the result for the low-frequency region $\omega \ll \omega_c$. Here we note that the LD part of the transducer is pre-biased just at the threshold current ($R=0$) by using the dark current of the HPT part as seen in Fig. 2. It is seen that RIN decreases monotonically with increasing P_{in} . When P_{in} is small, the LD part of the transducer is just above the threshold current and the amplified spontaneous and stimulated random emissions seriously affect the pure lasing mode (output signal light). When P_{in} increases, the optical power of the pure lasing mode increases and the influence of the random emission becomes small, therefore, RIN becomes small. We define here the noise equivalent power (NEP) as P_{in} at which RIN becomes 1, where the bandwidth $B=1$. It is found in Fig. 5 that the NEP of the transducer is about 30 pW.

TABLE 1 Numerical values used for noise calculation

Active layer volume	$V = 1.2 \times 10^{-10}$ [cm ³]
HPT cut-off frequency	$\omega_c/(2\pi) = 1 \times 10^6$ [Hz]
HPT gain at low frequency	$G_0 = 1000$
Carrier lifetime	$\tau_s = 3 \times 10^{-9}$ [s]
Photon lifetime	$\tau_{ph} = 1 \times 10^{-12}$ [s]
LD threshold current	$I_{th} = 42$ [mA]
Spontaneous emission factor	$\beta = 1 \times 10^{-5}$

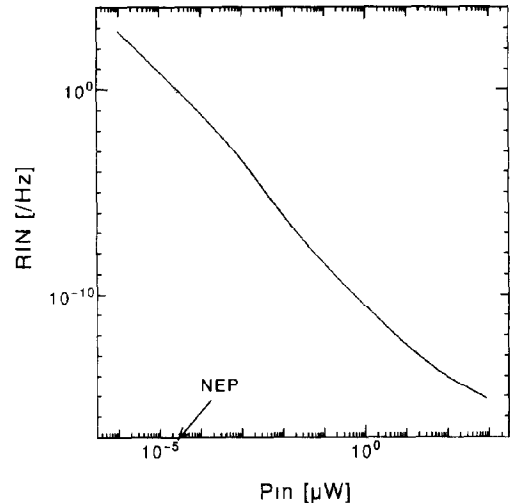


Fig. 5 RIN as a function of input light-signal power

Next, we consider the frequency dependence of RIN . The calculated results are shown in Fig 6 where P_{in} is taken as a parameter. RIN decreases once when the frequency exceeds 1 MHz and then increases rapidly. The decrease is due to the cut-off of the response of the HPT part, and the rapid increase is due to the enhancement of the noise caused by the relaxation oscillation of the LD part.

We next discuss the dependence of RIN on the conversion gain of the HPT. The calculated result is shown in Fig 7, where the gain G_0 of the HPT at the low-frequency region is taken as a parameter. It is seen in Fig 7 that RIN increases with decreasing G_0 . When G_0 is small, a small optical input P_{in} induces only a small current flow through the LD part. In this case,

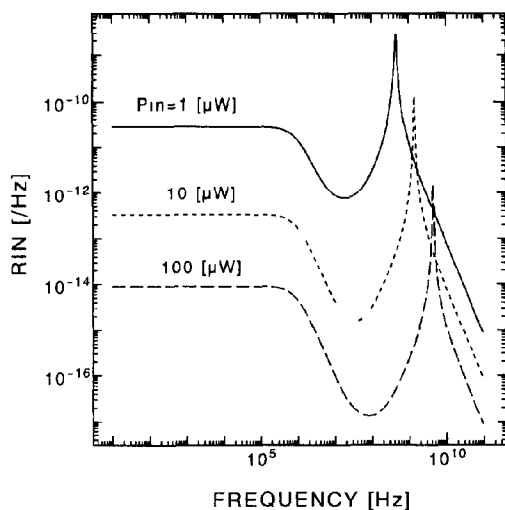


Fig 6 Frequency dependence of RIN , where the input light-signal power is taken as a parameter

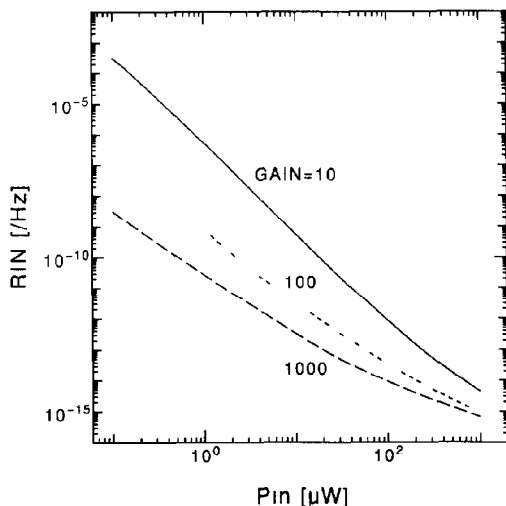


Fig 7 Conversion gain dependence of RIN

since the output signal power (the pure lasing mode) cannot be so large compared with the random emission, the noise increases. When P_{in} becomes large, however, the RIN difference between the larger and smaller G_0 cases becomes small. This is because the shot noise of the HPT becomes dominant for the total noise when P_{in} increases and the noise of the transducer with the larger-gain HPT increases rapidly.

Figure 8 shows RIN of the output light signal as a function of RIN of the input light signal, with P_{in} as a parameter. We consider here the case $P_{in} = 10 \mu\text{W}$, which is the typical input signal-power level. When the input RIN is larger than 5×10^{-13} , the output RIN is equal to the input RIN . This means that the RIN of the transducer is determined by the input noise itself. In this case, the noise figure, which is defined by the RIN ratio of the input and output light signals, becomes unity. However, when the input RIN is less than 5×10^{-13} , the output RIN is determined by the transducer itself, and the noise figure becomes worse. Therefore, it is very important to reduce the RIN of the transducer. One way to do this is to reduce the threshold current of the LD part, since this part is pre-biased by the dark current of the HPT and the pre-bias induces excess shot noise in the HPT part. Figure 9 shows RIN as a function of the threshold current I_{th} of the LD part. It can be seen that RIN indeed decreases with decreasing I_{th} .

From these discussions and some actual calculated numerical values, we may say that the transducer integrated with the HPT and the LD can be utilized as a relatively low-noise and high-sensitivity linear optical amplifier. Here we should note that the above discussions hold only when the LD part oscillates in a single longitudinal mode and the optical filter, with a

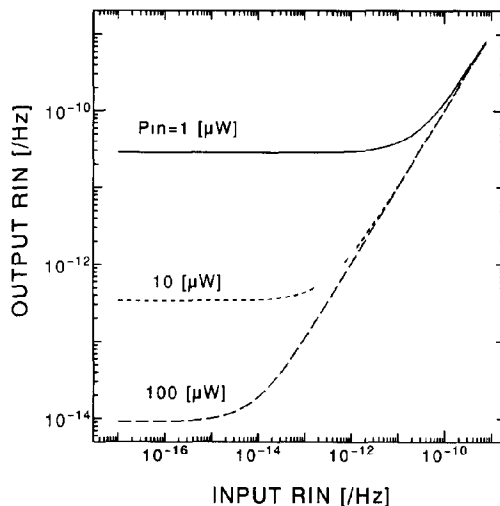


Fig 8 Relationship between output and input signal RIN s

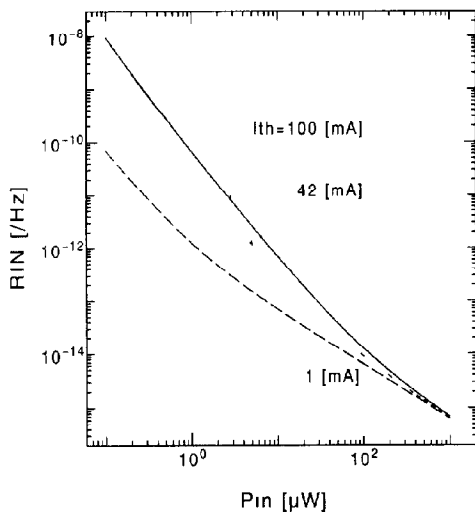


Fig 9 Threshold current dependence of RIN

very narrow bandwidth that can pass only the wavelength of the lasing mode, is put just after the output portion. The avalanche effect in the HPT part should also be considered. We are now trying to measure the noise of the transducer, and the results will be reported elsewhere.

5. Conclusions

A light-to-light transducer has been developed by vertical and direct integration of three HPTs and a laser diode. By the suppression of the internal optical feedback from the LD to the HPT, a quite good linearity between output and detecting optical powers has been obtained. A linear optical gain over 100 has been achieved for input light wavelengths of 0.75 to 1.25 μm . The maximum optical gain was 250 for a detecting optical wavelength of 0.92 μm , this is the highest ever reported for this type of light-to-light transducers.

The static intensity noise properties have also been discussed theoretically under ideal conditions. It has been derived that the noise equivalent power (NEP) is 30 pW and that the RIN for a typical input power level $\approx 10 \mu\text{W}$ is about 10^{-14} – 10^{-13} . Various other RIN properties dependent on the conversion gain of the HPT part and on the threshold current of the LD part have also been discussed.

Acknowledgements

The authors would like to thank Dr A. Wakahara for fruitful discussions. This work was supported in part by a Grant-in-Aid for Scientific Research on Priority Area 'Ultrafast and Ultraparallel Optoelectronics' (No. 05212211) from the Ministry of Education, Science and Culture of Japan.

References

- 1 A. Sasaki, Transducers from light to light, *Tech. Digest, 4th Int. Conf. Solid-State Sensors and Actuators (Transducers '87)*, Tokyo, Japan, June 2–5, 1987, pp. 3–10.
- 2 A. Sasaki, S. Metavikul, M. Itoh and Y. Takeda, Light-to-light transducer with amplification, *IEEE Trans. Electron Devices*, ED-35 (1988) 780–785.
- 3 S. Noda, T. Takayama, K. Shibata and A. Sasaki, High gain and very sensitive photonic switching device by integration of heterojunction phototransistor and laser diode, *IEEE Trans. Electron Devices*, ED-39 (1992) 305–312.
- 4 Y. Sakakibara, H. Higuchi, E. Omura, Y. Nakajima, Y. Yamamoto, K. Goto, K. Ikeda and W. Susaki, High-power 1.3 μm InGaAsP p-substrate buried crescent lasers, *IEEE J. Lightwave Technol.*, LT-3 (1985) 978–984.
- 5 Y. Yamamoto, AM and FM quantum noise in semiconductor lasers — Part I: theoretical analysis, *IEEE J. Quantum Electron.*, QE-19 (1983) 34–46.
- 6 F. H. Moneda, E. R. Chenette and A. Ziel, Noise in phototransistors, *IEEE Trans. Electron Devices*, ED-18 (1971) 340–346.
- 7 S. Noda, K. Kojima and K. Kyuma, Mutual injection-locking properties of monolithically integrated surface-emitting multiple-quantum-well distributed feedback lasers, *IEEE J. Quantum Electron.*, 26 (1990) 1883–1894.